

Brackish water treatment by ceramic TiO₂ low-pressure nanofiltration membranes

Hudaib B.¹, Hajarat R.², Al-Zoubi H.³ and Omar W.^{1,*}

¹Chemical Engineering Department, Faculty of Engineering Technology, Al-Balqa Applied University, Amman 11134, Jordan

²Mut'ah University, Department of Chemical Engineering, Al-Karak, Jordan

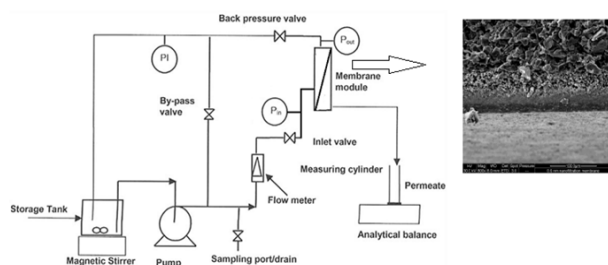
³Department of Chemical Engineering, College of Engineering, Al-Hussein Bin Talal University, P.O. Box 20, Ma'an, Jordan

Received: 10/10/2022, Accepted: 05/01/2023, Available online: 24/02/2023

*to whom all correspondence should be addressed: e-mail: waid.omar@bau.edu.jo

<https://doi.org/10.30955/gnj.004513>

Graphical abstract



Abstract

The application of ceramic Nanofiltration (NF) membrane in brackish water treatment is increasing due to strict water quality standards. The Ceramic NF membrane process is widely used nowadays and has replaced reverse osmosis (RO) membranes in many applications due to lower energy consumption and higher flux rates. This work aims to study tubular ceramic TiO₂ nanofiltration membrane separation performance for single and tertiary salt mixtures at low-pressure (2 bar). The results showed that the ions rejection is ordered as follows: R (Cl¹⁻) ion size > R calcium (Ca²⁺) ion size > R sodium (Na¹⁺) ion size > R magnesium (Mg²⁺) ion. The highest Cl¹⁻ rejection was 46%, the highest Ca²⁺ and Mg²⁺ rejection was 44%, and the highest Na¹⁺ rejection was 37%. The pure water flux through the investigated ceramic NF membrane for distilled water was calculated to be $5.29 \times 10^{-7} \text{ m}^3 \text{ s}^{-1} \text{ m}^{-2} \text{ bar}^{-1}$, and the flux was dropped down for the salt mixture feed to $2.56 \times 10^{-7} \text{ m}^3 \text{ s}^{-1} \text{ m}^{-2} \text{ bar}^{-1}$ due to the presence of salt particles in the feed.

Keywords: Ceramic membranes, nanofiltration, water purification, desalination, brackish water

1. Introduction

Water is one of the vital elements for plants, animals, and human beings; therefore, water availability for food production and residential uses is of paramount concern to governments and researchers, especially under the

pressure of the significant increase in the world population. Using alternative non-conventional water resources is the desalination researcher's goal worldwide (Hilal *et al.*, 2007). Water can be categorized according to salinity into four types: seawater, brackish water of high salinity, brackish water of low salinity, and potable water. Brackish water's salinity ranges between 1,000 and 15,000 ppm (Mohsen, 2007). Brackish water salinity is more than freshwater, but not as much as seawater. In principle, brackish water contains between 0.5 and 30 grams of salt per liter (Mohsen, 2007).

Jordan is classified among the ten poorest world countries in water, with less than 120 m³ estimated yearly water consumption per person. According to the water and irrigation ministry, the water deficits were about 419 million cubic meters (MCM) in 2019 and will reach about 490 MCM by 2025. Jordan's available total brackish water amount is about 219 MCM per year, with an average salinity of 1000-3000 ppm. The estimated ground brackish water is about 78 MCM per year, with an average salinity ranging from 1300 to 8028 ppm (Mohsen *et al.*, 1999).

Mohsen *et al.* (Mohsen *et al.*, 2007) stated that the available amount of brackish water in Jordan valley is about 80 MCM, which can be a potential water resource for irrigation if treated by economically feasible technologies. Alsarayreh *et al.* (Alsarayreh *et al.* 2017) investigated using a renewable energy source, such as solar energy, for brackish water desalting in Jordan Valley. They reported that applying photovoltaic (PV) energy systems for brackish water desalting in a single small-scale plant at the current electricity price is relatively high cost and not affordable for the farmers; however, it might be feasible for larger-scale desalination plants to supply reclaimed water for more than ten farms with governmental funding. The economic evaluation studies indicated that using PV-powered desalination systems for brackish water treatment from the government's perspective is economically feasible even for small-scale desalination plants.

In the same direction, Taha and Al-Sa'ed (Taha & Al-Sa'ed, 2017) investigated the viability of applying reverse

osmosis (RO) desalination system powered by solar energy to treat saline brackish water at the Marj Naajeh desalination plant in the Jordan Valley. An economic evaluation was benchmarked to traditional energy sources such as diesel generators and network electricity. The environmental impacts were also considered. The results recommended upgrading agricultural wells of different water capacities and quality. They also suggested that conducting additional research studies on the design, capacity, and efficiency of future desalination plants would be more beneficial.

Mohsen and Al-Jayyousi (Mohsen *et al.*, 1999) used multi-criteria analysis to evaluate various desalination methods. The evaluation criteria implemented were based on technical, economic, and environmental aspects. In addition, both the quality and quantity of different brackish waters were assessed. The investigation showed that RO desalination technology is ranked as the highest suitable for treating brackish waters, followed by electrodialysis (ED) as the second most successful desalination technology.

1.1. Desalination using nanofiltration membrane

Membrane technology has been extensively applied over the last decade for brackish water, wastewater, and seawater desalination due to its separation performance and low energy requirement (Schäfer *et al.*, 1998). Nanofiltration (NF) is a well-known process to separate salts from saline brackish waters. It uses membranes manufactured from organic materials and polymers with pore sizes ranging from 0.1 nm to 10 nm. Contrary to RO membranes that operate at high pressure and can reject all solutes in water, NF membranes are characterized by low operating pressures and the rejection of particular solutes according to their size and charge (Hilal *et al.* 2004). The membrane system generally consists of a pre-treatment process of the feed water before the primary NF process, which can be followed by a post-treatment process. Using NF membrane separation technology, purifying and desalting brackish waters is currently used as an alternative to traditional salt separation processes (Al-Qadami *et al.*, 2020; Al-Zoubi *et al.*, 2007; N Hilal *et al.*, 2004) to supply clean and secure water resources for agriculture. Recently, NF membranes were successfully used to treat brackish groundwater water found in South Tunisia (Kammoun *et al.*, 2020).

NF membranes are applied to separate salts from saline waters, surface water, and groundwater (Al-Harashsheh *et al.*, 2017). Surface water treatment using NF is a good option; however, the surface water usually has variable salt concentration due to rain dilution. Moreover, NF is an appropriate choice for eliminating organic matter (Hilal *et al.*, 2004). On the other hand, NF is more appropriate than RO for lime softening and separating naturally occurring organic carbon materials such as color and harmful side products (Van der Bruggen & Vandecasteele, 2003). Retentions higher than 90% using NF systems were found for multivalent ions, whereas monovalent ions retentions were about 60–70% (Hilal *et al.*, 2005; Schaep *et al.*, 1998). Another study implemented NF membranes as a

pre-treatment step for real seawater desalination using RO process in a pilot plant (Kaya *et al.*, 2020). The integrated system gave a reasonable rejection of seawater salts (97%) at 30 bar. According to the recent study by Suhalim *et al.* (Suhalim *et al.*, 2022), the separation mechanisms of ionic compounds in the polymeric NF membranes are due to size exclusion, Donnan exclusion, and dielectric exclusion.

NF membranes' application for water softening was studied and compared to other traditional techniques, such as pellet softening and granular activated carbon (Sombekke *et al.*, 1997). The results revealed that NF membranes have several advantages in terms of lower investment costs and productivity. A significant advantage of applying NF is its ability to remove all hardness cations. Hence, they are applicable when treating unnecessary side streams to decrease hardness to low levels. This can be achieved by splitting only a part of the feed water to be softened by the NF membranes, and the permeate is then mixed with the bulk flow stream. In contrast, when applying the precipitated lime softening process, the hardness could not be reduced to levels below 50 mg/L CaCO₃. This side stream softening is practically not attainable (Hilal *et al.*, 2004).

1.2. Ceramic nanofiltration membranes

Ceramic NF membranes are regarded as a good choice in many applications (Condom *et al.*, 2004; Radeva *et al.*, 2021; Zhu *et al.*, 2018); the separation of solutes from saline waters using ceramic Nanofiltration (CNF) membranes were extensively investigated (Sondhi *et al.*, 2003). Recently, CNF membranes have become a gradually favored option when treating salty water. CNF membranes have several advantages over other organic and polymeric NF membranes; chemical stability and the ability to operate at different extreme pH levels and high temperatures and pressures make these membranes more attractive for water treatment. Moreover, CNF membranes can resist vigorous backwashing and chemical cleaning, which help to control membrane fouling. The rejection of ions through CNF membranes is influenced by the concentration of salts and the feed water's pH. Correspondingly, trans-membrane pressure primarily affects ionic rejection (Skruzacek *et al.*, 2007; Van Gestel *et al.*, 2002b).

Many additives were used to modify NF membranes, including Al₂O₃, TiO₂, ZrO₂, and SiO₂. Of these, TiO₂ attracted attention due to its unique characteristics, e.g., higher chemical and physical stability, withstanding high temperatures, and long service life (Bhave, 1991; Guo *et al.*, 2018; Koutsonikolas *et al.*, 2010; Sekulić *et al.*, 2004; Zhang *et al.*, 2006).

Qi *et al.* (Qi *et al.*, 2012) used γ -Al₂O₃ modified CNF membranes, and the results showed less chemical stability in severe conditions, thus limiting their industrial applications. Benfer *et al.* (Benfer *et al.*, 2001) showed that the ZrO₂ NF membrane showed a rejection rate as high as 66.3% for SO₄²⁻. Cai *et al.* (Cai *et al.* 2015) modified

Pb/TiO₂ membranes via the colloidal sol-gel process and attained higher rejections of salts than undoped TiO₂ membranes.

Gestel *et al.* (Van Gestel *et al.*, 2002a, 2006) studied the stability of γ -Al₂O₃, TiO₂, and ZrO₂-modified CNF membranes in both acid and alkaline solutions. The γ -Al₂O₃ membranes results present less stability in an aqueous solution with (pH 3-11); however, the TiO₂ and ZrO₂ membranes showed high stability for pH values from (1 to 13)

TiO₂ is gaining more popularity in ceramic NF membrane improvement owing to its unique characteristics like super-hydrophilicity and high chemical stability (Lu *et al.*, 2016; Sekulić *et al.*, 2004). Many researchers have focused on the development of TiO₂-modified ceramic NF membranes. Titanium dioxide (TiO₂) nanoparticles are also employed in membranes to increase salt removal from water (Sakarkar *et al.*, 2021; Ursino *et al.*, 2018). The retention of charged and uncharged solutes and solvent permeability is the most crucial characteristic of membrane performance (Luo & Yinhua, 2013; Schäfer *et al.*, 1998; Wahab Mohammad & Sobri Takriff, 2003). More details about the fabrications of CNF membranes and their applications in the desalination process using membrane distillation techniques were reviewed by Tai *et al.* (Tai *et al.*, 2019).

Liang investigated the viability of using TiO₂ CNF membranes to treat an artificial brine experimentally (Liang, 2018). A laboratory-scale apparatus of two flat disc CNF membranes with different molecular weight cut-offs were applied to filtrate artificial brines at different concentrations of single salt or NaCl/Na₂SO₄ salts mixtures. The results indicated the low rejection of sulphate, chloride, and sodium ions. It was also realized that the sulphate rejection could be improved by decreasing ionic strength and adding sodium chloride according to the Donnan effect and co-ion competing. In addition, fouling problems were measured due to the drop in water permeability during the experiment. Moreover, the difference in molecular weight cut-off before and after brine filtration was considered an indication of membrane fouling.

Hudaib *et al.* (Hudaib *et al.*, 2019) investigated the separation performance of low-pressure tubular TiO₂-CNF membranes operating at 2 bar. The effect of the valences, type of ions, transmembrane pressure (TMP), and the Zeta potential of the membrane on the separation of ions was studied experimentally. A single and three salt mixtures of sodium chloride, sodium nitrate, and sodium sulphate were tested in the study. It was found that the rejection of ions is arranged in the order: sulphate ions > nitrate ions > chloride ions > sodium ions. The highest rejection ratios for sulphate, nitrate chloride and sodium ions were 62%, 51%, 42%, and 37%, respectively. In another study (Pérez-González *et al.*, 2015), a polymeric NF270 membrane was investigated to remove the SO₄²⁻ / Cl⁻ mixture. It was found that SO₄²⁻ rejection was in the 75-96% range and chloride rejections between 2% and 11%. However, when NaCl concentration is increased, the

rejection of SO₄²⁻ was reduced due to the decrease in the Donnan effect. Similar findings were reported by Krieg *et al.* (Krieg *et al.* 2005).

In another study by Reig *et al.*, the NF270 membrane was used to reject NH₄⁺ /NO₃ in a cross-flow apparatus, applying a spacer-filled feed channel of a rectangular geometry (Reig *et al.*, 2016). The membrane permeability to sodium ions was found to be more significant than to chloride ions because of an electric field that caused negative rejections of the trace nitrate anion. The existing electric field highly accelerated this. Another study shows that solute transport through an NF membrane pore depends on the sieving mechanism and the surface force interaction between the solute and the pore (Xu & Lebrun, 1999).

1.3. Irrigation water treatment

Although irrigation water contains ions such as Na⁺, Ca²⁺, and Mg²⁺, which are essential for the plant's growth, excessive amounts are harmful and can cause severe damage to the plants. High Na⁺ replaces Ca²⁺ and Mg²⁺ ions at the exchange complex, which carry a negative charge. This will negatively affect the soil's quality leading to soil structure deterioration, and the soil aggregates will be dispersed. In the long run, this will reduce the soil permeability for infiltration, initiating unfavorable growing conditions for plants. A critical factor that should be considered is the sodium absorption ratio (SAR) which is a sum of the Ca²⁺ and Mg²⁺ ions concentration divided by the concentration of Na⁺ ions. The higher the SAR, the lower the Na⁺ hazard. The soil infiltration rate can be decreased if the irrigation water is treated with a high SAR value and the salinity level is reduced to low or moderate. (Ayers & Westcot, 1985)

Unfortunately, magnesium ions concentration in the brackish water in Jordan is high and can cause nutrition disorders for the plants. The high magnesium (Mg²⁺) ions concentrations constrain plant growth and decrease crop harvest amounts. If Mg²⁺ dominates in the irrigation water, i.e., the concentration ratio Ca²⁺/Mg²⁺ < 1, the possible influence of sodium might be augmented, and plant nutrition might be disordered (Ayers & Westcot, 1985).

On the other hand, most of the brackish water in the Jordan Valley resources has a high chloride concentration, more than 10 meq/L, which is harmful to the fruit crops. For irrigation purposes, the chloride content should be less than 3 meq/L using sprinkler irrigation equipment. Although chloride has minor adverse impacts on soil, it can toxify the crops and accumulate in the leaves of lemon and other crops irrigated by high chloride contents brackish water. The adverse effects of chloride begin at 10 meq/L concentration, and higher concentrations of more than 3 meq/L in water using sprinkler irrigation will create a burn in the plants' leaves (Ayers & Westcot, 1985).

Therefore, this study aims to use Ceramic TiO₂ low-pressure NF membrane for single and tertiary salt mixtures in view of chloride removal of the brackish water desalination in Jordan. The efficiency and separation

performance for single and multivalent ions at low pressure, the effect of surface charge (at fixed pH), and its influence on the separation performance of the membrane were investigated to get the best conditions to enhance the separation performance of the NF membrane. Moreover, the effect of ionic strength on ionic rejection was tested.

2. Materials and methods

2.1. Saline water

In this experiment, samples of the saline water containing single salt and mixed salts of sodium chloride, magnesium chloride, and calcium chloride, with a concentration of 0.1 M, were used. All salts are obtained from Sigma-Aldrich, Germany. Both sodium hydroxide and hydrochloric acid (0.1 M) are used to control the solution pH. The membrane is cleaned by sodium hydroxide.

2.2. Ceramic nanofiltration membrane

A ceramic tubular TiO₂ Nanofiltration membrane (7.0 mm ID, 10.0 mm OD, 190 mm length and 0.9 nm mean pore radius) was obtained from inopor GmbH- Germany and used for water desalination. The hydrophilicity (contact angle) of the membrane measured by the supplier is about 42±2 °C.

The morphological structure of the used ceramic membrane was investigated using SEM analysis. Figure 1 shows the SEM image of the used membrane obtained by SEM (FEI Quanta 200, Purge, Czech Republic) and EDXS equipment (Amertek Inc., Paoli, PA, USA). The membrane layers (active and supporting) are clearly shown in Figure 1. A thicker skin layer is observed; therefore, higher rejection and lower permeate flux are expected.

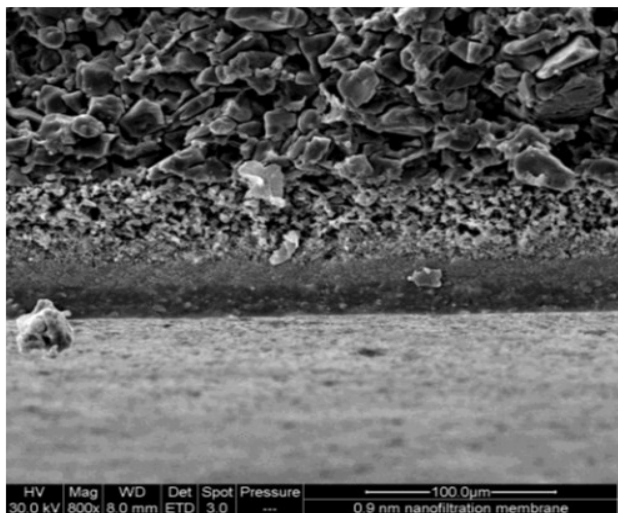


Figure 1 Ceramic NF membrane SEM image showing the active layer and support layer. (Scale bar: 100 μm)

2.3. Experimental set-up

The main components of the bench-scale membrane rig used in this experiment, as shown in (Figure 2) are a peristaltic pump with variable speed (type 603S, Watson-Marlow, UK), magnetic stirrer (RW20, IKAMAG, UK), tubular membrane module, glass container, pressure-relief valve, PVC-reinforced flexible piping, flexible

neoprene piping for the pump (Watson-Marlow, UK), flow-meter (Gemü Gebr Müller, Germany), pH/ORP controller (Oakton), Accumet pH/Ion/Conductivity meter (Fisher Scientific, Model 50), balance and stopwatch. The resultant solutions anion's concentration was measured using ion chromatography (Dionex DX600 Ion Chromatograph), and the cation concentration was measured by inductively coupled plasma atomic emission spectroscopy (ICP-AES).

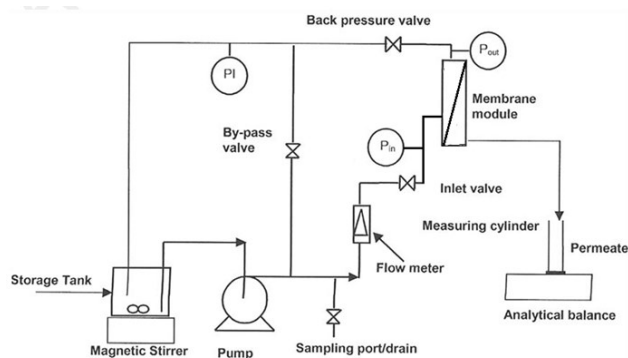


Figure 2 The bench-scale set-up used in this study

2.4. Experimental procedure

The separation performance of the investigated CNF membrane was studied by filtration of pure distilled water, then the single or tertiary salt solution, and finally, the distilled water to check the effect of the precipitation of the salt on the membrane surface. First, Distilled water permeated through the ceramic membrane at a constant inlet volumetric flow rate of $3.056 \times 10^{-5} \text{ m}^3/\text{s}$ (110 L/h). Then, the pressure inlet was increased from 0.3 bar to 2.0 bar, which gives transmembrane pressure (TMP) values between 0.2 to 1.9 bar. Next, the permeation experiments for salts were carried out for single and mixed salts. Single salt solutions of NaCl, MgCl₂, and CaCl₂ were prepared with 0.1 M concentration at a pH of around 7, while mixed solutions were prepared from the three salts together with 0.1 M concentration for each salt. For each experiment, the pressure was increased by 0.2 intervals every 30 minutes, and the collected permeate was continued for 25 minutes. After each experiment, the membrane was cleaned with distilled water many times; after that, it was cleaned with 0.1M NaOH solution for 1 hour and washed with distilled water continuously for 6 hours. The test was repeated three times for all permeation experiments, and the average was recorded.

2.5. TMP measuring and membrane rejection

The permeate flux through a porous membrane is described as the transmembrane pressure driving force (TMP), divided by (R) the resistance to mass transfer, and the permeate viscosity, μ (Field *et al.*, 1995).

$$J = \frac{TMP}{\mu R} \quad (1)$$

For distilled water filtration, R will represent the resistance to mass transfer associated with the clean membrane. During an experiment, the resistance to

permeation increases because of different mechanisms, like pore block, cake formation, and concentration polarization. In constant TMP operation, as R increases, the permeate flux declines, while, at constant flux operation, TMP increases as R increases (Taniguchi *et al.*, 2003). Characterizing nanofiltration membrane can be done by determining its critical flux. Below critical flux, no flux decline occurs with time, while above it, fouling can be observed (Miller *et al.*, 2014). There are two types of critical flux: strong critical flux and weak critical flux. TMP starts to deviate from the distilled water flux in strong critical flux, but the solution and distilled water membrane resistance are the same.

Moreover, in weak critical flux, flux values are lower than distilled water flux, where the membrane resistance for the solution is different from that of the distilled water, and the membrane resistance changes with the increasing flux after the critical flux is reached (Bacchin *et al.*, 2006; Field *et al.*, 1995). Field *et al.* (Field *et al.*, 1995) research provided specific observations of constant TMP and flux measurements. They observed low membrane fouling and total mass transfer resistance in constant flux experiments and high fouling and total mass transfer resistance in constant TMP experiments, possibly due to the rapid fouling at the beginning of constant TMP experiments.

The rejection (R) of the ceramic NF membrane of ion (i) is calculated by the following formula (Gerald *et al.*, 2008):

$$R = 1 - \frac{C_{i,p}}{C_{i,f}} \quad (2)$$

$C_{i,p}$ is the ion concentration in the permeate (mol/L), and $C_{i,f}$ is the ion concentration in the feed (mol/L).

While the TMP is estimated as follows (Piry *et al.*, 2008):

$$TMP = \left(\frac{P_{inlet} + P_{outlet}}{2} \right) - P_{permeate} \quad (3)$$

The pressure at the permeate side is usually assumed to be equal to zero, and hence the TMP would be as follows:

$$TMP = \left(\frac{P_{inlet} + P_{outlet}}{2} \right) \quad (4)$$

The water permeability, WP ($L \cdot h^{-1} \cdot m^{-2} \cdot bar^{-1}$), was estimated as follows (N Hilal *et al.*, 2005):

$$WP = \frac{V_p}{A \cdot t \cdot TMP} \quad (5)$$

Where V_p is the Volume of water permeate (L), A is effective membrane area (m^2), t is time (h), and TMP is the applied pressure (bar).

3. Results and discussion

3.1. Zeta potential measurement

The membrane surface charge was measured using the electrophoretic mobility of TiO_2 membrane powder derived from the membrane top layer (Guizard *et al.*, 1999). The experiments were run at pH ranging from 3 to 10 at room temperature (25 ± 0.50 °C). Sodium chloride

(NaCl) salt with 0.1M concentration was used. The pH of the solutions was adjusted by using 0.1M HCl and 0.1M NaOH. The crushed membrane was added to the prepared solution, and the zeta potential was measured. Different pH was used to understand the membrane properties and the salts' effect on membrane charge.

Figure 3 shows the results of membrane zeta potential at different pH values, which indicates that the membrane zeta potential is decreased as the pH increases. The iso-electric point (ISP) determines the membrane charge, which is considered the main parameter in justifying the ion's rejection behavior at a pH of about 4.5. Moreover, Figure 3 shows that as the pH increases, the membrane zeta potential decreases, and the higher the pH, the more negative membrane zeta potential is obtained. Luo & Yinhua, Mänttari *et al.*, and Szoke *et al.* further investigated the effect of pH on NF performance (Luo & Yinhua, 2013; Mänttari *et al.*, 2006; Szoke *et al.*, 2003).

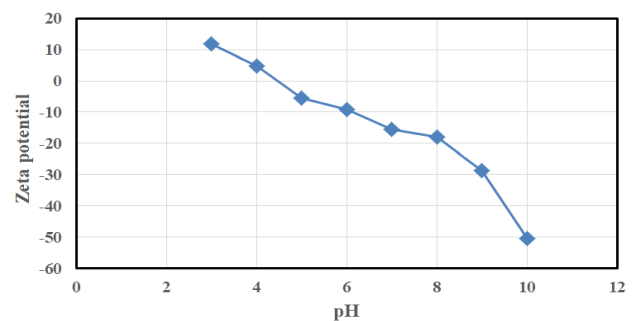


Figure 3 Surface zeta potential for TiO_2 NF membrane

3.2. Single salt rejection

Figure 4 shows that the rejection of Na^{1+} increases as TMP increases until it reaches the maximum value of 8% at 1.5 bar; then, it decreases and becomes negative, which means it passes freely through the membrane. The rejection of Cl^{-1} ions from NaCl solution is increased as the TMP increases; this may be due to the electrostatic repulsion interaction between the negative charges of the membrane and the Cl^{-1} ion. These results are consistent with many studies (Luo & Yinhua, 2013; Szoke *et al.*, 2003; Teixeira *et al.*, 2005). Figure 4 indicates that rejection of the Cl^{-1} sharply increases after 1.5 bar and reaches the highest rejection of Cl^{-1} , which is about 22% at a TMP of 1.9 bar. This sharp increase may result from the negative rejection of Na^{1+} , and the effects of the membrane charge and the Cl^{-1} cause more repulsion as no cations can neutralize part of the negative membrane charge. The electro-neutrality condition can clarify the low rejection of both Cl^{-1} and Na^{1+} ions. Both ions are diffused through the membrane to neutralize the charge on the permeate side.

In $MgCl_2$, the rejection of Cl^{-1} is higher than that of Mg^{2+} , as illustrated in Figure 5. This result may be explained by the electrostatic interaction between the membrane charge and ion charge or the so-called Donnan exclusion. The attraction between negative membrane charge and positive Mg^{2+} leads to the passage of Mg^{2+} ions more freely through the membrane than Cl^{-1} . While both

negative charges of Cl⁻¹ and membrane surface cause repulsion between the membrane and Cl⁻¹ to reject Cl⁻¹ and then back to the solution, other researchers obtained similar results (Labban *et al.*, 2017; Yaroshchuk, 2008).

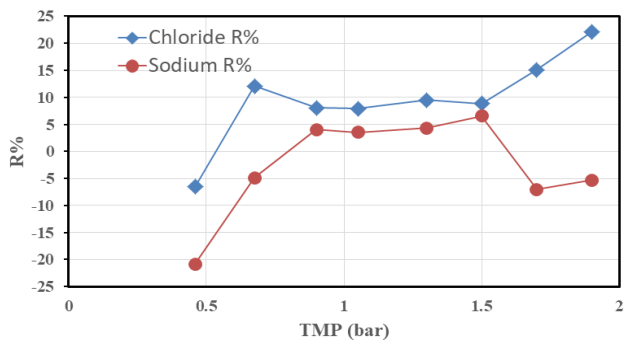


Figure 4 Relationship between rejection and TMP for Na and Cl ions at pH of 7

The rejections of Mg²⁺ are negative (except at the lowest TMP value, 0.3 bar). Similar results were reported by Yaroshchuk (Yaroshchuk, 2008). Negative rejection does not mean that mass (Mg²⁺ solute in this case) is being created; neither the mixture now has more Mg²⁺ ions than it initially started with. Negative rejection only means that the system has a higher concentration of Mg²⁺ in the permeate relative to the feed. In other words, negative rejection for a given ion species only occurs when more of that ion is in the smaller permeate volume relative to the much larger feed volume. In the same line, a membrane with negative rejection enhances the transport of that solute or ion across it (Yaroshchuk, 2008; Labban *et al.*, 2017, Hudaib *et al.*, 2019).

Besides, the bigger size of the Mg²⁺ ion compared to the Cl⁻¹ ion size plays a role in rejection, causing Mg²⁺ to pass more freely through the membrane (Pontalier *et al.*, 1997). The small rejection threshold might be due to TMP, which can overcome the charge force between the membrane and the ion charges and force the ions to pass through the membrane.

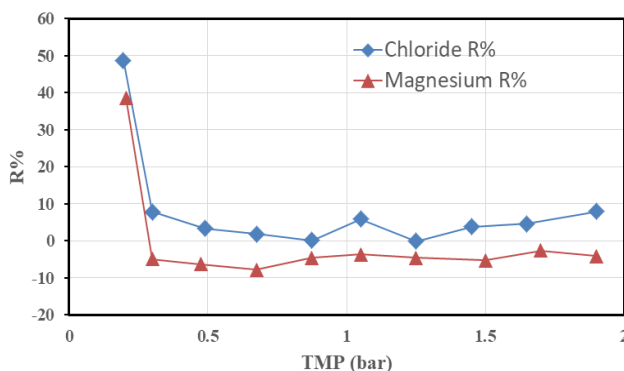


Figure 5 Relationship between rejection and TMP for Mg and Cl ions at pH of 7

As shown in Figure 6, the rejection behavior of CaCl₂ is the same as MgCl₂. The rejection of Ca²⁺ ions is lower than that of Cl⁻¹ ions. This may result from different charges of the ions and the membrane as well as the smaller size of Ca²⁺ compared to Cl⁻¹. The higher rejection ratio is about 37.4% and 40.0% for Ca²⁺ and Cl⁻¹, respectively. There is an

inverse relationship between the rejection of both ions and TMP. As the TMP increases, the rejection of both ions (Ca²⁺ and Cl⁻¹) decreases.

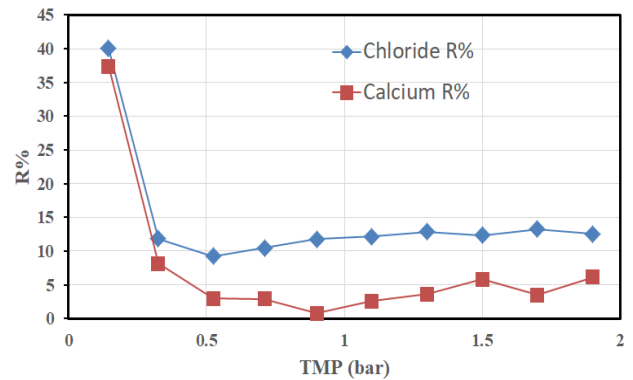


Figure 6 Relationship between rejection and TMP for Ca and Cl ions at pH 7.

3.3. Salts mixture rejection behavior

The TiO₂ ceramic NF membrane desalinates a solution mixture of three salts (NaCl, MgCl₂, and CaCl₂) at a pH of 7. For this experiment, the permeate flux through the membrane increases from 2.7 x 10⁻⁷ to 4.6 x 10⁻⁵ m³/m².s as the TMP increases. The results showed that the rejection of Cl⁻¹ is higher than Ca²⁺, which is higher than Mg²⁺ and Na¹⁺ (see Figure 7). Also, the rejection of all cations decreases after the first TMP (0.2 bar) and then remained almost constant as the TMP increases.

The highest rejection values (at 0.2 bar) are 43.1%, 42.1%, and 33.0% for Ca²⁺, Mg²⁺, and Na¹⁺ ions, respectively. Negative rejection values of Na¹⁺ mean that it permeated freely through the membrane. The rejection of Cl⁻¹ decreases after the first TMP and almost stays constant as the TMP increases.

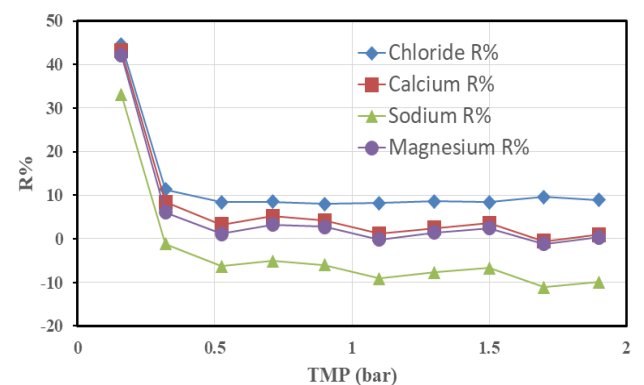


Figure 7 Relationship between rejection and TMP for Mg, Na, Ca, and Cl ions at pH of 7

The rejection of Cl⁻¹ is the highest, followed by Ca²⁺, then Mg²⁺ and Na¹⁺, which is negative after (0.3) TMP. All the rejection values sharply decrease at lower TMP, i.e., below 0.3 bar, almost constant or slightly varies after increasing the TMP over 0.3 bar with the same ranking. The higher rejection values of Cl⁻¹ are due to the repulsion of the negative charges of both Cl⁻¹ and the membrane, while the other three ions have a positive charge opposite to the membrane charge, which causes attraction between the membrane and the cations, allowing those

positive ions to permeate more freely through the membrane. In addition to the size of the cations playing a role in rejection, the sizes are arranged as follows (Cl^{-1}) ion size > calcium (Ca^{2+}) ion size > sodium (Na^{1+}) ion size > magnesium (Mg^{2+}) ion size. The sodium (Na^{1+}) ion size > magnesium (Mg^{2+}) ion size, but the charge of Mg^{2+} is double the charge of Na^{1+} , so the repulsion of magnesium is double that of Na. This filtration rejection (efficiency) will decrease with increasing the salt concentration. This conclusion was approved in our previous study (Al-Zoubi & Waid, 2009).

The low rejection values of the three investigated cations and Cl^{-} might be due to the electro-neutrality condition at both sides of the membrane, where ions permeate from the high concentration (feed side) to the low concentration (permeate side) to achieve the charge equilibrium condition.

A comparison of the ion's filtration from a single salt solution and a mixed salt solution shows that the rejection of Mg^{2+} from a mixed salt solution is higher than that of a single salt solution; it showed negative as the TMP increases more than 0.3 bar. The rejection of Ca^{2+} from a mixed salt solution is higher than that of a single salt solution, with positive rejection in both cases. The mixed solution makes the rejection of Na^{1+} negative and lower than that of the single salt solution. The rejection of the Cl^{-} ion in all cases is still the highest of all ions, while the rejection of Cl^{-} from calcium chloride is higher than that of magnesium chloride and sodium chloride mono solutions.

3.4. Permeate flux behavior

Pure water flux for the investigated membrane was found to increase linearly with the transmembrane pressure, as shown in Figure 8. The permeate flux vs. pressure was obtained initially for distilled water (distilled water 1), then it was calculated for the salt mixture (NaCl , MgCl_2 , and CaCl_2). After the salty water experiment, the membrane was cleaned using the following steps: Initially, the membrane was washed with distilled water many times to remove the salt ions from the membrane surface. After that, the membrane was cleaned with 0.1M NaOH solution for 1 hour, and finally, the membrane was washed with distilled water for 4 hours until the ions were removed. The permeate flux is estimated again for the distilled water (distilled water 2). The water permeabilities estimated from Eq.4 were 5.29×10^{-7} , 4.72×10^{-7} , and $2.56 \times 10^{-7} \text{ m}^3 \text{ s}^{-1} \text{ m}^{-2} \text{ bar}^{-1}$ for distilled water 1, salty water, and distilled water 2, respectively. The permeate flux increases with pressure due to the increase in solvent flux. Transport through the NF membrane can be explained in terms of convection and diffusion (N Hilal *et al.*, 2004); the water flux is higher at a higher pressure, and the contribution of diffusion becomes less important relative to convection.

On the other hand, the permeate flux of salty water was relatively low due to the salt particles' presence in the feed water, which obstructs the diffusion of permeate water through the surface of the NF membrane. The flux

of distilled water 2 was lower than that of distilled water 1 due to the precipitation of some of the salt particles over the membrane surface (concentration polarization), which occurred after carrying out a salt mixture's filtration of NaCl , MgCl_2 , and CaCl_2 (N Hilal *et al.*, 2004)

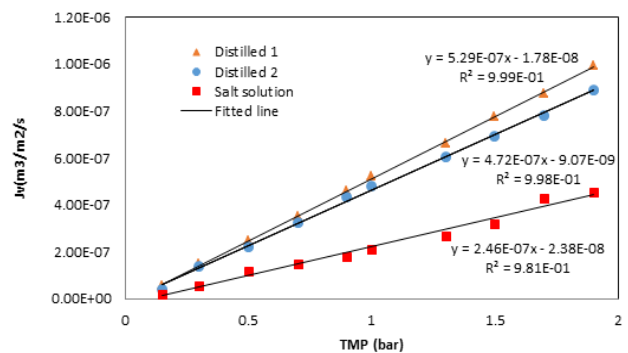


Figure 8 The permeate flux vs. pressure for distilled water 1, salty mixture (NaCl , MgCl_2 , and CaCl_2), and distilled water 2.

4. Conclusion

The objective of this study is to investigate the separation performance of the ceramic NF membrane of saline water solutions containing single and mixed salts of NaCl , MgCl_2 , and CaCl_2 under low pressure. The results showed that the rejections of Cl^{-} ions are always the highest due to the negative charge of both the chloride and the membrane. The rejection of Na^{1+} increased as TMP increased until it reached the maximum value of 8% TMP at 1.5 bar, then started to decrease and become negative, which means it passed freely through the membrane. While the rejection of calcium cations is positive, on the contrary, the rejection of magnesium cations is negative; that is, the membrane freely allows the cations to go through. As a result, the Cl^{-} ion has a higher rejection than the Ca^{2+} ion. The highest Ca^{2+} rejection was 43.1%, the highest Mg^{2+} rejection was 42.1%, and the highest Na^{1+} rejection was 33.0%. The highest Cl^{-} rejection was 44.6%. The sequence of rejection is (Cl^{-}) ion size > calcium (Ca^{2+}) ion size > sodium (Na^{1+}) ion size > magnesium (Mg^{2+}) ion size. The ion's size and the charge, and the value of the charges play an essential role in the rejection process. Based on the obtained results, a CNF membrane is potentially recommended to filtrate salty water with high Cl^{-} concentration.

Many combined processes were investigated for brackish water treatment to achieve the best rejections, such as using NF technology with RO to get optimal brackish water treatment (Cai *et al.*, 2020). Chen *et al.* used a dual-stage NF system to treat brackish water in the Binhai Area of Tianjin (with TDS > 12,000 mg/L); A quartz sand filter activated carbon and UF were used as a pre-treatment unit (Chen *et al.*, 2013).

However, in this study, authors investigated the use of a low-pressure NF process to study the way of rejecting different types of ions. Thus in future work, a combined cheap pre-treatment process will be investigated with the NF membrane used in this study.

References

- Al-Harabsheh M., Hussain Y.A., Al-Zoubi H., Batiha M. and Hammouri E. (2017). Hybrid precipitation-nanofiltration treatment of effluent pond water from phosphoric acid industry. *Desalination*, **406**, 88–97. <https://doi.org/10.1016/j.desal.2016.06.014>
- Al-Qadami E., Ahsan A., Mustafa Z., Abdurrasheed A., Yusof K W. and Shah S. (2020). Nanofiltration membrane technology and its applications in surface water treatment: A review. *Journal of Desalination and Water Purification*, **18**, 3–9.
- Alsarayreh A., Majdalawi M., and Bhandari R. (2017). Techno-Economic Study of PV Powered Brackish Water Reverse Osmosis Desalination Plant in the Jordan Valley. *The International Journal of Thermal & Environmental Engineering (IJTEE)*, **14**, 83–88. <https://doi.org/10.5383/ijtee.14.01.010>
- AlZoubi H. and Waid O. (2009). Rejection of salt mixtures from high saline by nanofiltration membranes. *Korean Journal of Chemical Engineering* **26**, 799–805. <https://doi.org/10.1007/s11814-009-0133-7>.
- Al-Zoubi H., Hilal N., Darwish N.A. and Mohammad A.W. (2007). Rejection and modelling of sulphate and potassium salts by nanofiltration membranes: neural network and Spiegler–Kedem model. *Desalination*, **206**(1), 42–60. <https://doi.org/10.1016/j.desal.2006.02.060>
- Ayers R.S., and Westcot D.W. (1985). Water quality for agriculture. FAO Irrigation and drainage paper 29 Rev. 1. *Food and Agricultural Organization. Rome*, **1**, 74.
- Bacchin P., Aimar P., and Field R.W. (2006). Critical and sustainable fluxes: Theory, experiments and applications. *Journal of Membrane Science*, **281**(1), 42–69. <https://doi.org/10.1016/j.memsci.2006.04.014>
- Benfer S., Popp U., Richter H., Siewert C., and Tomandl G. (2001). Development and characterization of ceramic nanofiltration membranes. *Separation and Purification Technology*, **22–23**, 231–237. [https://doi.org/10.1016/S1383-5866\(00\)00133-7](https://doi.org/10.1016/S1383-5866(00)00133-7)
- Bhave R. (1991). *Inorganic Membranes Synthesis, Characteristics and Applications* (first edit). Van Nostrand Reinhold. <https://doi.org/10.1007/978-94-011-6547-1>
- Cai Y., Wang Y., Chen X., Qiu M., and Fan Y. (2015). Modified colloidal sol–gel process for fabrication of titania nanofiltration membranes with organic additives. *Journal of Membrane Science*, **476**, 432–441. <https://doi.org/10.1016/j.memsci.2014.11.034>
- Cai Y.; Yang X., and Schäfer A.I. (2020). Removal of Naturally Occurring Strontium by Nanofiltration/Reverse Osmosis from Groundwater. *Membranes*, **10**, 321.
- Chen X., Zhao H., Wang L., and Fu X. (2013). Application of two stages nanofiltration in desalting of high degree brackish water. *Membr. Sci. Technol.*; **33**:63–67.
- Condom S., Larbot A., Younsi S A., and Persin M. (2004). Use of ultra- and nanofiltration ceramic membranes for desalination. *Desalination*, **168**, 207–213. <https://doi.org/10.1016/j.desal.2004.06.189>
- Field R.W., Wu D., Howell J.A., and Gupta B.B. (1995). Critical flux concept for microfiltration fouling. *Journal of Membrane Science*, **100**(3), 259–272. [https://doi.org/10.1016/0376-7388\(94\)00265-Z](https://doi.org/10.1016/0376-7388(94)00265-Z)
- Geraldes V., Pinho M., Fonseca C., and Duarte E. (2008). Spiral-wound Module Nanofiltration of Surface River Water. *E-Water*.
- Gestel T.V., Vandecasteele C., Buekenhoudt A., Dotremont C., Luyten J., Leysen R., Van der Bruggen B., and Maes G. (2002b). Salt retention in nanofiltration with multilayer ceramic TiO₂ membranes. *Journal of Membrane Science*, **209**(2), 379–389. [https://doi.org/10.1016/S0376-7388\(02\)00311-3](https://doi.org/10.1016/S0376-7388(02)00311-3)
- Gestel T.V., Kruidhof H., Blank D.H.A., and Bouwmeester H.J.M. (2006). ZrO₂ and TiO₂ membranes for nanofiltration and pervaporation: Part 1. Preparation and characterization of a corrosion-resistant ZrO₂ nanofiltration membrane with a MWCO<300. *Journal of Membrane Science*, **284**(1), 128–136. <https://doi.org/10.1016/j.memsci.2006.07.020>
- Gestel T.V., Vandecasteele C., Buekenhoudt A., Dotremont C., Luyten J., Leysen R., Van der Bruggen B., and Maes G. (2002a). Alumina and titania multilayer membranes for nanofiltration: preparation, characterization and chemical stability. *Journal of Membrane Science*, **207**(1), 73–89. [https://doi.org/10.1016/S0376-7388\(02\)00053-4](https://doi.org/10.1016/S0376-7388(02)00053-4)
- Guizard C., Palmeri J., Amblardm P., Diaz J., and Lasserre J. (1999). No Title. *Basic Transport Phenomena of Aqueous Electrolytes in Sol-Gel Derived Meso and Microporous Ceramic Oxide Membranes", Proceedings of the Ninth CIMTEC of World Ceramic Congress on Application to Commercial Ceramic Nanofilter Performance*, 202–205.
- Guo H., Zhao S., Wu X., and Qi H. (2018). Fabrication and characterization of TiO₂/ZrO₂ ceramic membranes for nanofiltration. *Microporous and Mesoporous Materials*, **260**, 125–131. <https://doi.org/10.1016/j.micromeso.2016.03.011>
- Hilal N, Al-Zoubi H., Darwish N.A., Mohamma A.W., and Arabi M.A. (2004). A comprehensive review of nanofiltration membranes: Treatment, pre-treatment, modelling, and atomic force microscopy. *Desalination*, **170**(3), 281–308. <https://doi.org/10.1016/j.desal.2004.01.007>
- Hilal N, Al-Zoubi H., Mohammad A.W., and Darwish N.A. (2005). Nanofiltration of highly concentrated salt solutions up to seawater salinity. *Desalination*, **184**(1), 315–326. <https://doi.org/10.1016/j.desal.2005.02.062>
- Hilal N, Al-Zoubi H., Darwish N.A., and Mohammad A.W. (2007). Performance of nanofiltration membranes in the treatment of synthetic and real seawater. *Separation Science and Technology*, **42**(3), 493–515. <https://doi.org/10.1080/01496390601120789>
- Hudaib B., Hajarat R., and Liu Z. (2019). *The Ceramic TiO₂ Low-Pressure Nano-Filtration Membrane Separation Behavior for Single and Mixed Ion Salt Solutions*.
- Kammoun M., Gassara S., Palmeri J., Amar R., and Deratani A. (2020). Nanofiltration performance prediction for brackish water desalination: case study of Tunisian groundwater. *Desalination and Water Treatment*, **181**, 27–39. <https://doi.org/10.5004/dwt.2020.25100>
- Kaya C., Jarma Y.A., Guler E., Kabay N., Arda M., and Yükse M. (2020). Seawater Desalination by using Nanofiltration (NF) and Brackish Water Reverse Osmosis (BWRO) Membranes in Sequential Mode of Operation. *Journal of Membrane Science and Research*, **6**(1), 40–46. <https://doi.org/10.22079/jmsr.2019.107844.1264>
- Koutsonikolas D.E., Kaldis S.P., Sklari S.D., Pantoleonos G., Zaspalis V.T., and Sakellaropoulos G.P. (2010). Preparation of

- highly selective silica membranes on defect-free γ -Al₂O₃ membranes using a low temperature CVI technique. *Microporous and Mesoporous Materials*, **132**(1), 276–281. <https://doi.org/10.1016/j.micromeso.2010.03.007>
- Krieg H.M., Modise S.J., Keizer K., and Neomagus H.W.J.P. (2005). Salt rejection in nanofiltration for single and binary salt mixtures in view of sulphate removal. *Desalination*, **171**(2), 205–215. <https://doi.org/10.1016/j.desal.2004.05.005>
- Labban O., Liu C., Chong T.H., and Lienhard V.J.H. (2017). Fundamentals of low-pressure nanofiltration: Membrane characterization, modeling, and understanding the multi-ionic interactions in water softening. *Journal of Membrane Science*, **521**, 18–32. <https://doi.org/10.1016/j.memsci.2016.08.062>
- Liang F. (2018). *Ceramic nanofiltration membrane for ions separation from ion exchange brine: effect of ionic strength and salts on ionic rejection* [Delft University of Technology]. <http://resolver.tudelft.nl/uuid:0b2c3d31-ce49-4b24-8648-b496fd9af472>
- Lu Y., Chen T., Chen X., Qiu M., and Fan Y. (2016). Fabrication of TiO₂-doped ZrO₂ nanofiltration membranes by using a modified colloidal sol-gel process and its application in simulative radioactive effluent. *Journal of Membrane Science*, **514**, 476–486. <https://doi.org/10.1016/j.memsci.2016.04.074>
- Luo J., and Yinhu W. (2013). Effect of pH and salt on nanofiltration – A critical review. *Journal of Membrane Science*, **438**, 18–28. <https://doi.org/10.1016/j.memsci.2013.03.029>
- Mänttari M., Pihlajamäki A., and Nyström M. (2006). Effect of pH on hydrophilicity and charge and their effect on the filtration efficiency of NF membranes at different pH. *Journal of Membrane Science*, **280**(1), 311–320. <https://doi.org/10.1016/j.memsci.2006.01.034>
- Miller D.J., Kasemset S., Paul D.R., and Freeman B.D. (2014). Comparison of membrane fouling at constant flux and constant transmembrane pressure conditions. *Journal of Membrane Science*, **454**, 505–515. <https://doi.org/10.1016/j.memsci.2013.12.027>
- Mohammad A.W., and Takriff M.S. (2003). Predicting flux and rejection of multicomponent salts mixture in nanofiltration membranes. *Desalination*, **157**(1), 105–111. [https://doi.org/10.1016/S0011-9164\(03\)00389-8](https://doi.org/10.1016/S0011-9164(03)00389-8)
- Mohsen M. (2007). Water strategies and potential of desalination in Jordan. *Desalination*, **203**, 27–46. <https://doi.org/10.1016/j.desal.2006.03.524>
- Mohsen M.S., and Al-Jayyousi O.R. (1999). Brackish water desalination: an alternative for water supply enhancement in Jordan. *Desalination*, **124**(1), 163–174. [https://doi.org/10.1016/S0011-9164\(99\)00101-0](https://doi.org/10.1016/S0011-9164(99)00101-0)
- Pérez-González A., Ibáñez R., Gómez P., Urtiaga A.M., Ortiz I., and Irabien J.A. (2015). Nanofiltration separation of polyvalent and monovalent anions in desalination brines. *Journal of Membrane Science*, **473**, 16–27. <https://doi.org/10.1016/j.memsci.2014.08.045>
- Piry A., Kühnl W., Grein T., Tolkach A., Ripperger S., and Kulozik U. (2008). Length dependency of flux and protein permeation in cross-flow microfiltration of skimmed milk. *Journal of Membrane Science*, **325**(2), 887–894. <https://doi.org/10.1016/j.memsci.2008.09.025>
- Pontalier P.Y., Ismail A., and Ghoul M. (1997). Mechanisms for the selective rejection of solutes in nanofiltration membranes. *Separation and Purification Technology*, **12**(2), 175–181. [https://doi.org/10.1016/S1383-5866\(97\)00047-6](https://doi.org/10.1016/S1383-5866(97)00047-6)
- Qi H., Zhu G., Li L., and Xu N. (2012). Fabrication of a sol-gel derived microporous zirconia membrane for nanofiltration. *Journal of Sol-Gel Science and Technology*, **62**. <https://doi.org/10.1007/s10971-012-2711-0>
- Radeva J., Roth A.G., Göbbert C., Niestroj-Pahl R., Dähne L., Wolfram A., and Wiese J. (2021). Hybrid Ceramic Membranes for the Removal of Pharmaceuticals from Aqueous Solutions. *Membranes*, **11**(4). <https://doi.org/10.3390/membranes11040280>
- Reig M., Licon E., Gibert O., Yaroshchuk A., and Cortina J.L. (2016). Rejection of ammonium and nitrate from sodium chloride solutions by nanofiltration: Effect of dominant-salt concentration on the trace-ion rejection. *Chemical Engineering Journal*, **303**, 401–408. <https://doi.org/10.1016/j.cej.2016.06.025>
- Sakarkar S., Muthukumar S., and Jegatheesan V. (2021). Tailoring the Effects of Titanium Dioxide (TiO₂) and Polyvinyl Alcohol (PVA) in the Separation and Antifouling Performance of Thin-Film Composite Polyvinylidene Fluoride (PVDF) Membrane. In *Membranes*, **11**(4). <https://doi.org/10.3390/membranes11040241>
- Schaep J., Van der Bruggen B., Uytterhoeven S., Croux R., Vandecasteele C., Wilms D., Van Houtte E., and Vanlerberghe F. (1998). Removal of hardness from groundwater by nanofiltration. *Desalination*, **119**(1), 295–301. [https://doi.org/10.1016/S0011-9164\(98\)00172-6](https://doi.org/10.1016/S0011-9164(98)00172-6)
- Schäfer A.L., Fane A.G., and Waite T.D. (1998). Nanofiltration of natural organic matter: Removal, fouling and the influence of multivalent ions. *Desalination*, **118**(1), 109–122. [https://doi.org/10.1016/S0011-9164\(98\)00104-0](https://doi.org/10.1016/S0011-9164(98)00104-0)
- Sekulić J., Ten Elshof A., and Blank D. (2004). A Microporous Titania Membrane for Nanofiltration and Pervaporation. *Advanced Materials*, **16**, 1546–1550. <https://doi.org/10.1002/adma.200306472>
- Skuzacek J.M., Tejedor M.I., and Anderson M.A. (2007). NaCl rejection by an inorganic nanofiltration membrane in relation to its central pore potential. *Journal of Membrane Science*, **289**(1), 32–39. <https://doi.org/10.1016/j.memsci.2006.11.034>
- Sombekke H.D.M., Voorhoeve D.K., and Hiemstra P. (1997). Environmental impact assessment of groundwater treatment with nanofiltration. *Desalination*, **113**(2), 293–296. [https://doi.org/10.1016/S0011-9164\(97\)00144-6](https://doi.org/10.1016/S0011-9164(97)00144-6)
- Sondhi R., Bhawe R., and Jung G. (2003). Applications and benefits of ceramic membranes. *Membrane Technology*, **2003**, 5–8. [https://doi.org/10.1016/S0958-2118\(03\)11016-6](https://doi.org/10.1016/S0958-2118(03)11016-6)
- Suhaim N.S., Kasim N., Mahmoudi E., Shamsudin I.J., Mohammad A.W., Mohamed Zuki F., and Jamari N.L. (2022). Rejection Mechanism of Ionic Solute Removal by Nanofiltration Membranes: An Overview. In *Nanomaterials*, **12**(3). <https://doi.org/10.3390/nano12030437>
- Szoke S., Patzay G., and Weiser L. (2003). Characteristics of thin-film nanofiltration membranes at various pH-values.

- Desalination*, **151**(2), 123–129. [https://doi.org/https://doi.org/10.1016/S0011-9164\(02\)00990-6](https://doi.org/https://doi.org/10.1016/S0011-9164(02)00990-6)
- Taha M., and Al-Sa`ed R. (2017). Application potential of small-scale solar desalination for brackish water in the Jordan Valley, Palestine. *International Journal of Environmental Studies*, **75**(1), 214–225. <https://doi.org/10.1080/00207233.2017.1403759>
- Tai Z.S., Aziz M., Othman M.H., Mohamed Dzhahir M.I.H., Hashim N., Koo K., Hubadillah S., Ismail A., Rahman M., and Jaafar J. (2019). Ceramic Membrane Distillation for Desalination. *Separation & Purification Reviews*, **49**(4), 317–356. <https://doi.org/10.1080/15422119.2019.1610975>
- Taniguchi M., Kilduff J.E., and Belfort G. (2003). Modes of Natural Organic Matter Fouling during Ultrafiltration. *Environmental Science & Technology*, **37**(8), 1676–1683. <https://doi.org/10.1021/es020555p>
- Teixeira M., Rosa M., and Nyström M. (2005). The role of membrane charge on nanofiltration performance. *Journal of Membrane Science*, **265**, 160–166. <https://doi.org/10.1016/j.memsci.2005.04.046>
- Ursino C., Castro-Muñoz R., Drioli E., Gzara L., Albeirutty M.H., and Figoli A. (2018). Progress of Nanocomposite Membranes for Water Treatment. *Membranes*, **8**(2). <https://doi.org/10.3390/membranes8020018>
- Van der Bruggen B., and Vandecasteele C. (2003). Removal of pollutants from surface water and groundwater by nanofiltration: overview of possible applications in the drinking water industry. *Environmental Pollution*, **122**(3), 435–445. [https://doi.org/10.1016/S0269-7491\(02\)00308-1](https://doi.org/10.1016/S0269-7491(02)00308-1)
- Xu Y., and Lebrun R.E. (1999). Comparison of nanofiltration properties of two membranes using electrolyte and non-electrolyte solutes. *Desalination*, **122**(1), 95–105. [https://doi.org/10.1016/S0011-9164\(99\)00031-4](https://doi.org/10.1016/S0011-9164(99)00031-4)
- Yaroshchuk A.E. (2008). Negative rejection of ions in pressure-driven membrane processes. *Advances in Colloid and Interface Science*, **139**(1), 150–173. <https://doi.org/https://doi.org/10.1016/j.cis.2008.01.004>
- Zhang H., Quan X., Chen S., and Zhao H. (2006). Fabrication and characterization of silica/titania nanotubes composite membrane with photocatalytic capability. *Environmental Science & Technology*, **40**(19), 6104–6109. <https://doi.org/10.1021/es060092d>
- Zhu B., Due M., Dumée L., Merenda A., des Ligneris E., Kong L., Hodgson P., and Gray S. (2018). Short Review on Porous Metal Membranes—Fabrication, Commercial Products, and Applications. *Membranes*, **8**, 83. <https://doi.org/10.3390/membranes8030083>